

Beyond a Hartree–Fock description of crystalline solids: the case of lithium hydride

Silvia Casassa · Migen Halo · Lorenzo Maschio ·
Carla Roetti · Cesare Pisani

Received: 21 September 2006 / Accepted: 13 October 2006 / Published online: 13 December 2006
© Springer-Verlag 2006

Abstract It is shown that a local MP2 approach can be conveniently adopted as a first step towards the post-Hartree–Fock description of crystalline solids. The relation of a new periodic MP2 code (CRYSCOR) to a classical Hartree–Fock program (CRYSTAL) is outlined. As an illustration, the case of LiH, a prototypical ionic crystal, is treated in some detail by analyzing the effect of the perturbative correction on equilibrium geometry, lattice energy and electron distribution (X-ray structure factors, directional Compton profiles), with reference to experimental data.

Keywords Crystalline solids · Local correlation · MP2 · Density matrix · Lithium hydride

1 Introduction

Computer codes using one-electron Hamiltonians, either based on density functional theory (DFT) or on the Hartree–Fock (HF) approximation, provide nowadays efficient techniques for solving the many-electron problem for periodic systems. The former approach is by far preferred in applications. This is because HF is affected by a systematical error related to its neglect of dynamic correlation between electron motions. Conversely, owing to clever formulations of the exchange–correlation term in the Kohn–Sham Hamiltonian, DFT provides usually very accurate results as far as geometries and cohesion energies are concerned, at

comparable or lower cost; the evaluation of energy derivatives with respect to nuclear coordinates or to external perturbations is also easier, due to the absence of non-local terms in the Hamiltonian. On the other hand, the limitations of DFT are well known. The most disturbing one, in principle, is the lack of systematic rules for improving indefinitely the quality of the DFT solution. From a practical viewpoint, the fact that standard DFT cannot describe dispersion interactions between distant parts of the system [1] makes this approach unsuitable for many important solid state applications. An alternative approach is then needed, at least for calibrating DFT parameterizations.

Molecular quantum chemistry provides an astounding variety of ab initio wave-function-based methods for evaluating electronic correlation effects; they usually adopt the HF solution Φ^{HF} as a reference starting point. Extending these methodologies from finite to periodic systems has been the object of a lot of important work in the past and in recent years (see for instance Ref. [2] for an extended review). For such efforts to result in an efficient scheme, two conditions must be satisfied: first, that a good reference HF solution for the crystal is available; secondly, that the correlation technique may be easily adapted to periodic systems and its costs scale smoothly with the size of the repetitive unit.

Computational techniques for the accurate determination of Φ^{HF} for simple periodic systems have been available for almost two decades now, mainly as a result of work in our group, in collaboration with the Daresbury laboratory [3,4]. The evolution of those early techniques has resulted in a powerful computer code, CRYSTAL, which in its present version [5] is one of the few existing computational tools capable of providing not only DFT solutions, but also accurate HF ones for

S. Casassa · M. Halo · L. Maschio · C. Roetti · C. Pisani (✉)
Dipartimento Chimica IFM and Centre of Excellence
NIS (Nanostructured Interfaces and Surfaces),
Università di Torino, via P. Giuria 5, 10125 Torino, Italy
e-mail: cesare.pisani@unito.it

a variety of crystalline systems, and is undoubtedly the best tested among them [6]. Concerning the latter of the two pre-requisites for setting up an efficient post-HF computer code for crystals, the local correlation method in Pulay, Meyer and Saeb's formulation [7–9], and implemented in the molecular MOLPRO code [10], seems ideally suited. It is particularly convenient for large molecular systems since it scales linearly with the molecular size (N), at least asymptotically. Order N formulations of some of the most popular correlation techniques have been implemented and shown to perform very efficiently: Rayleigh–Schrodinger perturbation techniques in second (MP2) [11] and higher (MP4) [12] orders, coupled cluster theory confined to singles and doubles (CCSD) [13] or including triple corrections [CCSD(T)] [14], etc.

Taking advantage of this favorable situation, a research project has been started in our laboratory in collaboration with the group of Professor Schütz (one of the main MOLPRO's authors) at the University of Regensburg, aimed at implementing a new computer code, CRYSCOR, for the evaluation of post-HF effects on the properties of periodic, non-conducting systems. The idea is to reformulate the local correlation approach for the case of translational invariance, and to exploit as far as possible algorithms, technology and knowhow from the two reference codes, MOLPRO and CRYSTAL: this objective is made easier by the fact that both codes adopt a basis set of atomic orbitals (AO) $\chi_\alpha(\mathbf{r})$, which are in turn expressed as a linear combination of Gaussian type orbitals (GTO). As a first step in this direction, we have chosen to concentrate on MP2, the lowest level of post-HF perturbation theory; progress in this direction has been documented in a preceding paper [2]. It may be questioned whether the effort required to implement such a low-order correlation scheme is worthwhile. We think it is, for different reasons. In the first instance, many aspects of the machinery (definition of the local orthonormal functions, exploitation of translational and point symmetry, basis set calibration, efficient calculation of two-electron integrals and so on) can be implemented and checked at the MP2 level and carried on, almost unchanged, to higher levels of approximation. Secondly, MP2 describes rather accurately dispersive interactions, certainly better (both from a fundamental and a practical viewpoint) than DFT-based methods [15]. The semi-empirical “Grimme correction” [16–18] can also be used for correcting MP2 energies, which has been shown to improve impressively, at zero cost, the agreement with experimental correlation energies.

Energy (and related quantities: equilibrium geometries, energy derivatives with respect to external perturbations, etc.) is not the only property that is affected

by correlation effects and that deserves consideration and comparison with experimental results. In a recent paper [19] it was argued that determinations of the one-electron density matrix of crystalline systems, $\gamma_1(\mathbf{r}, \mathbf{r}')$, based on directional Compton profiles (CP) and X-ray structure factors (XSF), could be useful to assess the quality of computational techniques which take electron correlation effects into account. A scheme was there outlined for evaluating the correlation correction to the Hartree–Fock one-electron density, starting from the solution obtained for the periodic system at a perturbative MP n level. The case of crystalline lithium hydride was there indicated as specially suitable for this check, due to the abundance of high quality experimental data, and to the exceptional simplicity of its electronic structure.

We have chosen precisely LiH for documenting in this article some aspects of the present status of the CRYSCOR project. In Sect. 2 we first provide a brief resume of the periodic–local MP2 (P-LMP2) technique as implemented in CRYSCOR with emphasis given to computational aspects. The approximate estimate of the correlation correction to $\gamma_1^{\text{HF}}(\mathbf{r}, \mathbf{r}')$ is also described; it is shown how the effects of this correction on the calculated CPs and XSFs can be obtained rather straightforwardly, by means of the same routines used in CRYSTAL for the evaluation of those quantities at a non-correlated level. The transfer of information from CRYSTAL to CRYSCOR and vice versa is documented. Section 3 presents the LiH calculations. We first describe the computational choices adopted. Attention is given to those settings, which dictate the accuracy of the P-LMP2 correction, and to the approximations adopted in order to estimate the changes in the density matrix. The results are discussed with reference to the available experimental information and to the previous HF studies.

2 Theory and techniques

As anticipated in the introduction, the Pulay, Meyer and Saeb's approach is adopted here [7–9], suitably generalized to periodic systems, and based on a local representation of the occupied and virtual HF subspaces. Functions in the former set are obtained via a unitary transformation of the set of canonical orbitals by maximizing a pre-defined localization functional. In the present context, symmetry-adapted Wannier functions (SAWF) provided by the CRYSTAL program are used for this purpose [20,21]. The general function of this orthonormal set is indicated as $\phi_i(\mathbf{r})$ or simply $|i\rangle$. The virtual subspace is spanned by the non-orthogonal, linearly dependent set of the projected atomic orbitals

(PAO), obtained by applying to the general AO, $\chi_\alpha(\mathbf{r})$, the projector onto the virtual space: $\hat{Q} = \hat{1} - \sum_i |\mathbf{i}\rangle\langle\mathbf{i}|$. The general PAO is indicated as $\tilde{\chi}_\alpha(\mathbf{r})$ or simply $|\mathbf{a}\rangle$. In a periodic context, the indices $\mathbf{i}(\mathbf{j}, \mathbf{k}, \dots)$ and $\mathbf{a}(\mathbf{b}, \mathbf{c}, \mathbf{d}, \dots)$, which identify SAWFs and PAOs, respectively, are in fact double indices: $i\mathcal{L}, \dots a\mathcal{A}, \dots$ the first specifying the shape of the function, and the second the crystal cell to which it belongs.

The first order perturbative correction to the HF wavefunction may be written as a combination of *contravariant* doubly excited zero-spin configurations:

$$|\Psi^{(1)}\rangle = \sum_{\mathbf{ij}} \sum_{\mathbf{ab}} T_{\mathbf{ab}}^{\mathbf{ij}} |\Phi_{\mathbf{ij}}^{\mathbf{ab}}\rangle. \quad (1)$$

The unknown excitation amplitudes $T_{\mathbf{ab}}^{\mathbf{ij}}$ are determined through an iterative procedure, by imposing that all “residuals” $R_{\mathbf{ab}}^{\mathbf{ij}}$ are zero:

$$R_{\mathbf{ab}}^{\mathbf{ij}} = K_{\mathbf{ab}}^{\mathbf{ij}} + \sum_{\mathbf{cd}} \left\{ F_{\mathbf{ac}} T_{\mathbf{cd}}^{\mathbf{ij}} S_{\mathbf{db}} + S_{\mathbf{ac}} T_{\mathbf{cd}}^{\mathbf{ij}} F_{\mathbf{db}} + \right. \\ \left. - S_{\mathbf{ac}} \sum_{\mathbf{k}} \left(F_{\mathbf{ik}} T_{\mathbf{cd}}^{\mathbf{kj}} + T_{\mathbf{cd}}^{\mathbf{ik}} F_{\mathbf{kj}} \right) S_{\mathbf{db}} \right\}. \quad (2)$$

Here, $K_{\mathbf{ab}}^{\mathbf{ij}} = (\mathbf{ia}|\mathbf{jb})$ is the two-electron “exchange” integral; $F_{\mathbf{ik}}$ and $F_{\mathbf{ac}}$ are elements of the Fock operator in the WF or PAO representation, respectively; $S_{\mathbf{ac}}$ is the overlap between PAOs. Full exploitation of translational and point symmetry of the crystal permits us to confine the problem to an irreducible set of SAWF pairs, $(i\mathcal{O}; j\mathcal{J})$, of which the former belongs to the zero cell.

An essential notion of local correlation techniques, whereby the short-range character of dynamic correlation is exploited, is that of *domain* of any localized occupied orbital (SAWF, in the present case). Roughly speaking, each domain comprises the set of atoms which contribute significantly to the SAWF owing to a Mulliken-like criterion and to some pre-selected threshold [22]. A PAO is said to belong to a given domain, if the AO from which it is generated is associated with an atom in that domain; otherwise it is “external” to it. The *distance* $d_{\mathbf{ij}}$ between two SAWFs (\mathbf{i}, \mathbf{j}) is next defined as the minimum distance between any two atoms in the respective domains. The “locality Ansatz” is now introduced according to which amplitudes $T_{\mathbf{ab}}^{\mathbf{ij}}$ in Eq. 1 are negligible, either if the SAWFs \mathbf{i}, \mathbf{j} are very distant ($d_{\mathbf{ij}} > D_{\max}$), or if any of the PAOs \mathbf{a}, \mathbf{b} is external to both SAWF domains. Due to this Ansatz and to the local character of the Fock and overlap matrices, the computational cost asymptotically scales proportionally to the size N of the irreducible part of the repetitive unit.

In practical crystalline applications, the pre-factor of such a linear dependence on N is usually much larger than in standard molecular applications: in fact, because of the very compact nature of most three-dimensional periodic structures, huge numbers of two-electron K integrals must be calculated as a four-index transformation from the basic analytical integrals over AOs. A way out of this difficulty can be obtained by a systematic use of “density fitting” techniques [23,24], which reduce the problem to a three-index transformation of relatively simple integrals. The adaptation of this approach to periodic systems introduces enormous savings in the computational effort and is currently implemented in CRYSCOR [25,26]. For K integrals involving distant SAWF pairs, multipolar approximations can be used conveniently, which consist in estimating $K_{\mathbf{ab}}^{\mathbf{ij}}$ as the Coulomb interaction between the two product distributions, $(\mathbf{i} \times \mathbf{a})$ and $(\mathbf{j} \times \mathbf{b})$, each expressed as a combination of point multipoles [2].

The evaluation of the amplitudes through the annihilation of all residues $R_{\mathbf{ab}}^{\mathbf{ij}}$ (see Eq. 2) allows the second order energy *per cell* of the periodic system to be estimated according to the formula:

$$E_2 = \sum'_{i,j\mathcal{J}} \left\{ \sum'_{c\mathcal{C}, d\mathcal{D}} K_{d\mathcal{D}, c\mathcal{C}}^{i0, j\mathcal{J}} \left(2T_{d\mathcal{D}, c\mathcal{C}}^{i0, j\mathcal{J}} - T_{c\mathcal{C}, d\mathcal{D}}^{i0, j\mathcal{J}} \right) \right\}, \quad (3)$$

the prime to the summations meaning that they are confined to sets of indices satisfying the locality Ansatz. The estimate E_g of the correlation energy proposed by Grimme [16,17] and based on the consideration that the MP2 expression overestimates triplet with respect to singlet excitations differs from the one above in the substitution of the combination: $\left(2T_{d\mathcal{D}, c\mathcal{C}}^{i0, j\mathcal{J}} - T_{c\mathcal{C}, d\mathcal{D}}^{i0, j\mathcal{J}} \right)$ with: $\left[(a^g + b^g) T_{d\mathcal{D}, c\mathcal{C}}^{i0, j\mathcal{J}} - a^g T_{c\mathcal{C}, d\mathcal{D}}^{i0, j\mathcal{J}} \right]$. The values $a^g = 0.333$ and $b^g = 1.2$ are adopted here for the Grimme parameters.

The fact that an expression (Eq. 1) is available for the first order perturbative correction to the HF wavefunction suggests that estimates can be obtained of changes induced by correlation effects on the electron distribution. The one-electron density matrix $\gamma_1(\mathbf{r}, \mathbf{r}')$ contains a lot of information in this respect. It was pointed out in Ref. [19] that this fact is particularly relevant for periodic systems, where high quality information about γ_1 can be obtained from experimental determinations of X-ray structure factors and directional Compton profiles [27]. It is however not possible to obtain directly γ_1 as the expectation value of the related operator $\hat{P}_1^{\mathbf{r}, \mathbf{r}'}$ over $\alpha(\Phi^{\text{HF}} + \Psi^{(1)})$ (α being a normalization factor): this is because the resulting expression is not size-consistent,

and for an infinite system it would provide $\gamma_1(\mathbf{r}, \mathbf{r}') = \gamma_1^{\text{HF}}(\mathbf{r}; \mathbf{r}')$. In order to bypass this difficulty, a *locally correlated wavefunction* is defined, as obtained by adding to the HF solution only excitations where one of the two SAWFs is in the zero cell, but using for them the amplitudes from the P-LMP2 calculation. It can be viewed in a sense as the result of an “embedding” calculation, where electrons are allowed to correlate their motions in the zero cell and its neighborhood but are imposed to stay in their HF state far from it. There is more than that, however: for instance, the amplitudes include the effect of dispersive interactions up to infinite distance. The local MP2 correction to the HF one-density $\gamma'_{\text{loc}}^{\text{MP2}}(\mathbf{r}; \mathbf{r}')$ can be obtained from there, which coincides with that of the individual molecule in a molecular crystal in the limit of infinite values of the lattice parameters. Finally, a size-consistent periodic expression of the MP2 correction to the HF one-density can be worked out, which is conveniently expressed in terms of the AOs (see Ref. [19] for details):

$$\gamma'^{\text{MP2}}(\mathbf{r}; \mathbf{r}') = \sum_{\mu, \mathcal{M}, \nu, \mathcal{N}} P'_{\mu\mathcal{O}; \nu\mathcal{N} \in \mathcal{M}}^{\text{MP2, AO}} \chi_{\mu}(\mathbf{r} - \mathbf{R}_{\mathcal{M}}) \times \chi_{\nu}(\mathbf{r}' - \mathbf{R}_{\mathcal{N}}). \quad (4)$$

It is thus possible to calculate the corrections to the observable quantities of interest (electron density, momentum density, Compton profiles, autocorrelation function, X-ray structure factor, etc.) by simply feeding the corresponding subroutines of CRYSTAL with $P'^{\text{MP2, AO}}$ instead of $P^{\text{HF, AO}}$.

The general scheme of the exchange of information between CRYSTAL and CRYSCOR is outlined in Fig. 1. From a very concise information on the geometry of the system, a description of the basis set adopted, and from a few input parameters that determine the accuracy of the computation, CRYSTAL performs a complete symmetry analysis and calculates the SCF-HF (or DFT) solution. All geometry and symmetry information, the Fock and density matrix, the canonical eigenvalues and eigenvectors are stored on disk for use by the PROPERTIES code, which is an essential part of the CRYSTAL suite of programs. PROPERTIES calculates on request a number of quantities of interest: among these, the SAWFs can be obtained and stored on a disk, which are an essential input requirement for CRYSCOR. The latter program also gets from CRYSTAL the basis set, the Fock and HF density matrix in the AO representation and the geometrical characterization of the system. After solving the MP2 equations, CRYSCOR may determine the $P'^{\text{MP2, AO}}$ matrix. This is fed to the PROPERTIES program in the same format as $P^{\text{HF, AO}}$ (dashed arrows in Fig. 1), so allowing the

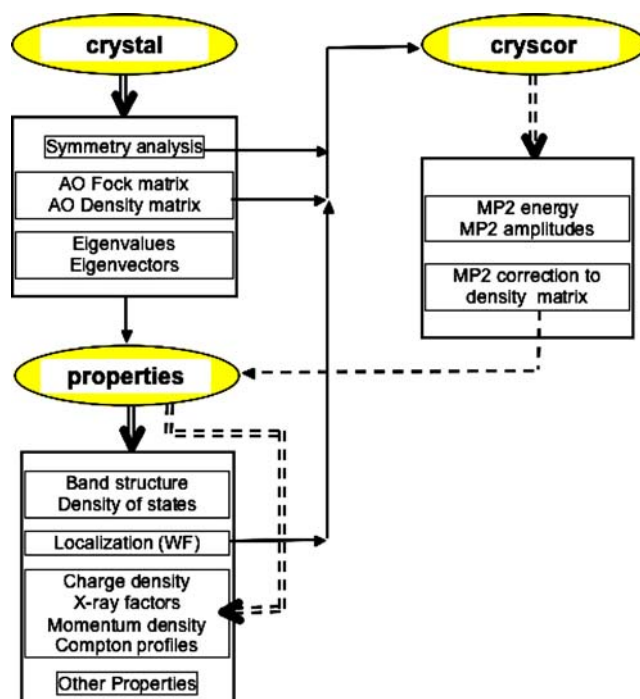


Fig. 1 Scheme of the transfer of information between CRYSTAL and CRYSCOR. Continuous and dashed arrows convey HF and MP2 information, respectively

re-calculation of all those quantities which only depend on the one-electron density matrix.

3 An MP2 study of lithium hydride

3.1 Computational aspects

In the rest of this paper, we present computations concerning crystalline LiH in order to illustrate some aspects of the present capabilities of the CRYSTAL–CRYSCOR suite of codes. This system has attracted widespread attention from experimentalists and theoreticians (see the comprehensive review by Islam [28] and the recent DFT study by Lebègue et al. [29]) because it may be considered the prototype of extreme ionic bonding, and because it is exceedingly simple: two nuclei and four electrons per unit cell, and a highly symmetric, face-centered cubic (fcc) structure. In particular, old but very accurate X-ray structure factors [30], and high quality CP data, both average [31] and directional [32,33], have been available since long. Over 20 years ago, these data were compared with the theoretical HF results obtained with the CRYSTAL program [34,35], or following the Adams–Gilbert–Kunz prescription [35–38], and the agreement was generally quite satisfactory. Ample

reference will be made in the following to our comprehensive HF study of that system [34].

The variationally optimized, extended basis set (EBS) adopted there is the reference one for the present work and will be indicated here as A. It comprises three s and one p shells on H, and two s and one p shells on Li; they are all single GTFs, except for the two 1s AOs resulting from the contraction of five and six GTFs for H and Li, respectively. The set A has been complemented with single-GTF d shells either on H alone (set B) or both on H and Li (set C). As shown below, the three sets provide almost equivalent HF results, while differences are evident at a correlated level. The use of more extended basis sets would create problems in the HF-SCF part due to the risk of quasi-linear-dependence among the Bloch functions, with no advantage on the quality of the HF solution. Work is in progress aimed at allowing the use of a “dual” basis set—the former for defining the HF occupied manifold, the latter including additional functions to improve the description of the virtual HF space. In all cases (HF, P-LMP2, “Grimme”), the calculated cohesive energies E_{coh} were corrected for the basis set superposition error (BSSE) following the standard counterpoise technique [39], and the equilibrium geometries were calculated using the BSSE-corrected E_{coh} values.

Standard tolerances were adopted for the HF calculations, both concerning truncation of lattice sums and k -space sampling. In all cases the P-LMP2 treatment was restricted to valence electrons, as is usual in this kind of calculations: the correlation effects between the core electrons are not likely to be affected significantly by the participation of atoms in molecular or crystalline structures, and in any case, the variational basis set adopted is not fit to describe such effects. As a consequence, we are left here with two correlated electrons per cell, which means that just one SAWF type $\phi_{\mathcal{J}}$ is determined by the LOCALI part of the CRYSTAL code. $\phi_{\mathcal{J}}$ is almost the same for the three basis sets because it only depends on the HF solution. As expected, it is very well localized about the H nucleus (its Mulliken population on H varies from 1.01 to 1.02 for the different basis sets) and is much more compact than the HF solution of the free hydride ion (the spatial extension $[\int d\mathbf{r} |\phi(\mathbf{r})|^2 r^2]^{1/2}$ of the two distributions about their center is 1.06 and 1.59 Å, respectively).

Let us now provide some details on the setting of the computational parameters for the P-LMP2 calculations. First, in order to apply the locality Ansatz, the SAWF domain must be defined. By default, we have assigned to each SAWF a 19-atom domain comprising the H^- ion on which it is centered, its 6 nearest neighbors Li^+ ions and the 12 second-neighbor H^- ions. A “small-domain”

setting, which includes only the first seven ions, and a “minimal-domain” setting, confined to the central H^- ion, were also considered for purposes of comparison. The value of D_{max} (distance between SAWFs beyond which pair interactions are disregarded) has been typically set to 12 Å. Extrapolation of the results to infinite distance ($D_{\text{max}} = \infty$) is possible, as shown below. If all the involved K integrals are calculated exactly, the corresponding step becomes the true bottleneck of the whole procedure. The time required is critically dependent on the threshold adopted for truncating the tails of SAWFs and PAOs: in the expansion of those functions as a linear combination of AOs, all terms are disregarded for which the absolute value of the expansion coefficient is less than a preselected value t^{coe} . With the choice here adopted, $t^{\text{coe}} = 0.001$, which provides rather accurate results (see for details Ref. [2]), and with $D_{\text{max}} = 12$ Å, the time required for a single energy point with basis set A on a 3 GHz PC [Intel Xeon (TM)] is approximately 140 h (5.8d). The multipolar technique can however be used safely when $d_{ij} > 8$ Å, which reduces the time to 55 h. Finally, if the density fitting approximation is used for closeby pairs, the cost is reduced to 30 min (52 min for basis set C) with no essential loss of accuracy.

The set of detors which defines the *locally correlated wavefunction* (see Sect. 2) comprises all bi-excited configurations $\Delta^{\text{loc}} = \{\mathcal{O}; \mathcal{G} | a; b\}$, where the WF in \mathcal{G} either coincides with that in \mathcal{O} or in one of the 12 lattice vectors \mathcal{G}_i of the star closest to the origin; a (and b) designs the general local orbital resulting from orthonormalization of the set of all PAOs on the 19 atoms closest to the origin, after eliminating the quasi-linear dependent combinations of PAOs (those corresponding to eigenvalues of the overlap matrix less than 0.001). The transformations described in Ref. [19] were then performed, and the elements of the matrix $P^{\text{MP2, AO}}$ (see Eq. 4) were determined, so allowing us to estimate the effects of the correlation correction on various quantities of interest.

3.2 Results and discussion

The results reported in Table 1 and Fig. 2 show the influence of the approximation scheme and the computational setting adopted on the cohesive energy of LiH, calculated with respect to the free ions treated in each case in the same approximation, and on the equilibrium value of the lattice parameter. In spite of the much better tolerances and of the more adequate treatment of the Madelung potential, the present HF results obtained with the reference set A are very close to those reported more than 20 years ago [34] (total energy -0.806187

Table 1 Calculated cohesive energy (Ha), lattice parameter (Å) and bulk modulus (GPa) of LiH

Basis set	HF			HF + MP2			HF + Grimme		
	E_{coh}	a_0	B_0	E_{coh}	a_0	B_0	E_{coh}	a_0	B_0
A	0.3423	4.126	27.7	0.3463	4.064	32.2	0.3444	4.086	31.0
B	0.3423	4.124	27.8	0.3477	4.040	32.3	0.3458	4.062	30.4
C	0.3425	4.121	28.3	0.3482	4.026	34.4	0.3462	4.055	32.6

Cohesive energies are corrected for the respective BSSE. The different basis sets and computational methods are described in the text. The experimental values (see text) are $E_{\text{coh}} = 0.3469$ Ha, $a_0 = 4.083$ Å, $B_0 = 32.1$ GPa

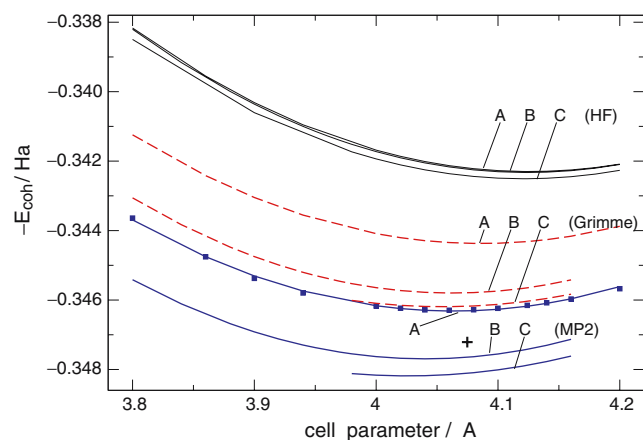


Fig. 2 Cohesive energy dependence on lattice parameter for different approximations (continuous thin lines HF; continuous thick lines HF+MP2; dashed lines HF+Grimme) and different basis sets (A, B, C, as indicated). The thick cross indicates the experimental values of cohesive energy and lattice parameter. For the HF+MP2-A case, the calculated points are marked to show the quality of the fitting curves

and -0.806289 Ha, respectively); they are not changed very much by the addition of the d functions on the two atomic species. The HF cohesive energy per cell is the same in all cases within 0.2 mHa, and is consistently lower than the experimental value [40] by about 4.3 mHa (~ 11 kJ mol $^{-1}$); the lattice parameter is also hardly affected and is larger than that observed by about 0.04 Å ($\sim 1\%$). The basis set choice affects to a larger

extent the MP2 results, as expected. It is apparent that convergence with respect to basis set quality has not yet been reached: work, to allow the use of better basis sets, is in progress, as stated in Sect. 3.1. The MP2 cohesive energy is larger than the HF one by 4.2 – 5.9 mHa, so overcorrecting the estimated correlation error. The calculated lattice parameter becomes shorter than the HF one by 0.06 – 0.08 Å, again exaggerating the correction. For both quantities, “better” basis sets provide larger MP2 corrections. Concerning the bulk modulus, quite recent and accurate volume versus pressure measurements for LiD at 300 K by Besson et al. [41], fitted to a first-order Murnaghan equation of state [42], give $B_0 = 32.1 \pm 0.3$ GPa. The same equation has been used for fitting the calculated data, and the results are reported in Table 2. The HF estimate is below the experimental value, probably because the calculated equilibrium interionic distance is too long. The MP2 correction gives slightly too large B_0 values. The values calculated with the Grimme formula for the three quantities are intermediate between the HF and MP2 results though closer to the latter; in general, this correction appears to provide a better agreement with the experiment.

It has however been pointed out by several authors that in crystalline structures composed of light atoms like LiH the calculated values of lattice parameter and bulk modulus should be corrected for zero point vibrations: the latter contribute in fact a volume-dependent term to the energy, which can be determined from the knowledge of the phonon dispersion as a function of

Table 2 Intra-SAWF correlation energy ($E_{\text{O}}^{\text{MP2}}$) and Lennard–Jones parameter (C_6) as a function of various computational settings.

Basis set	A			B			C		
	Standard	Small	Minimal	Standard	Small	Minimal	Standard	Small	Minimal
$E_{\text{O}}^{\text{MP2}}$ (% of E_2)	–0.02186 (76.6)	–0.021681 (79.6)	–0.02151 (84.0)	–0.02390 (76.5)	–0.02367 (79.4)	–0.02345 (83.5)	–0.02403 (75.5)	–0.02379 (78.2)	–0.02345 (83.2)
C_6	0.303	0.194	0.146	0.308	0.195	0.147	0.309	0.196	0.147

The percentage contribution of $E_{\text{O}}^{\text{MP2}}$ to the total MP2 energy per cell, E_2 is also indicated. As explained in the text, standard, small and minimal SAWF domains comprise 19, 7 and 1 atom, respectively. $E_{\text{O}}^{\text{MP2}}$ is given in Ha, C_6 in Ha Å $^{-6}$

volume: $E^{\text{ZP}}(V) = 1/2 \sum_{i,\mathbf{q}} \hbar \omega_i(\mathbf{q}, V)$. In order to estimate this zero-point (ZP) correction, Lebègue et al. [29] employed the E^{ZP} dependence on V obtained theoretically for LiH and LiD by Roma et al. [43] using density functional perturbation theory in a local density approximation and taking anharmonic effects into account. We have followed the same criterion for calculating the effect of the ZP correction on the results obtained with the C basis set. The corrected estimates of the lattice parameter ($a_0^{\text{ZP}}/\text{\AA}$) and of the bulk modulus ($B_0^{\text{ZP}}/\text{GPa}$) of LiH for the three computational methods are: 4.22 and 23.0 (HF); 4.12 and 27.0 (HF+MP2); 4.16 and 25.0 (HF+Grimme), respectively. The same technique cannot be applied to LiD (for which the best bulk modulus measurements are available [41]) because the corresponding data are not explicitly provided by Roma et al. [43]. However, from a comparison of the ZP correction to the bulk modulus of LiH and LiD reported by those authors, the three B_0^{ZP} values just quoted above for LiH can be estimated to be, in the LiD case: 24.1, 28.5, 26.5 GPa, respectively.

These results show that ZP corrections are important for crystalline LiH and LiD, and they seem to bring the MP2 results in closer agreement with the experiment.

The MP2 energy per cell, E_2 , can be usefully partitioned into “pair interaction energies” $E_{ij\mathcal{J}}^{\text{MP2}}$, by summing all the terms in Eq. 3 associated with excitations from a given $(i0, j\mathcal{J})$ SAWF pair in curly brackets. A parallel expression is obtained for $E_{ij\mathcal{J}}^{\text{g}}$. This partition allows us to obtain more detailed information on the various contributions to the correlation energy. In the present case, with just one SAWF per cell, the indices i and j can be dropped.

Table 2 reports the values of the only intra-SAWF contribution, $E_{\mathcal{O}}^{\text{MP2}}$, for different computational settings. It is seen that the correlation between the two electrons in the same hydride ion represents in all cases more than three-quarters of the whole E_2 . The percentage becomes larger with decreasing domain size, while it does not vary much with the basis set.

If the locality Ansatz holds true, inter-SAWF pair interactions must go rapidly to zero when the distance $d_{\mathcal{J}} = |\mathbf{R}_{\mathcal{J}}|$ between their centers becomes large. Figure 3 reports a log–log plot of $E_{\mathcal{J}}^{\text{MP2}}$ versus $d_{\mathcal{J}}$ for three different choices of the domain size. As expected, a very good Lennard–Jones-like $-C_6(d_{\mathcal{J}})^{-6}$ dependence of the pair interaction energy on distance is observed. Notice that points from calculations with different lattice parameters fall on the same straight line. The results of Fig. 3 are obtained with basis set A, but those for the two other basis sets are very similar. Table 2 reports the best fit values of C_6 as resulting from the available data in the interval $6 \text{\AA} < d_{\mathcal{J}} < 12 \text{\AA}$. A marked

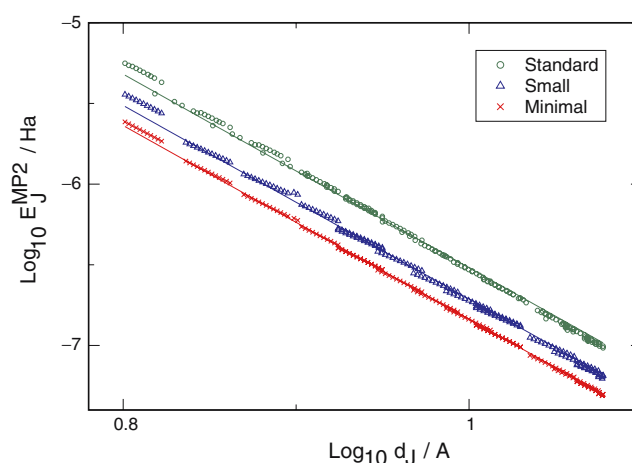


Fig. 3 Log–Log plot of the pair interaction energy ($E_{\mathcal{J}}^{\text{MP2}}/\text{Ha}$) versus the distance between the centers of the two SAWFs ($d_{\mathcal{J}}/\text{\AA}$) for basis set A and three domain sizes: standard (19 atoms, circles), small (7 atoms, triangles) and minimal (1 atom, crosses). The three straight lines are best fit lines with slope -6

dependence from domain size is confirmed, while the basis set effects are comparatively much smaller. These C_6 values can be compared to the experimental ones for He (0.036), Ne (0.193) and Ar (2.39), in the same units. Once C_6 is known, the contribution $\Delta E(d_{\text{max}})$ to the MP2 energy per cell of dispersive forces from all pairs at distances $d_{\mathcal{J}} > d_{\text{max}}$ is easily calculated: $\Delta E(d_{\text{max}}) = -4\pi C_6 / (3V_{\text{cell}}) \times (d_{\text{max}})^{-3}$. By substituting values, this residual contribution can be estimated to be about -50μ Hartree when $d_{\text{max}} = 12 \text{\AA}$. The procedure just outlined is easily generalized to the case where different SAWFs are present in each cell and permits extrapolation to an infinite distance. While the contribution from very distant pairs to the cohesion energy is negligible in the present case, it may become important in the presence of very polarizable ions or molecules.

The (valence-only) MP2 correction to the one-density in the AO representation, $P_{\mu\mathcal{O};\nu\mathcal{N}}^{\text{MP2, AO}}$ (see Eq. 4) was calculated as described in the previous section. It permits us to evaluate the redistribution of electrons due to correlation effects. A first indication is provided by the Mulliken analysis of the electronic populations reported in Table 3. With respect to the HF approximation, p and d AOs play a more important role in both species after the MP2 correction, and the system becomes slightly less ionic. This is mainly due to a decrease of the s population on H; closer analysis shows that it is only the most diffuse s AO on H which is depopulated.

Figure 4 reports the MP2 correction to the charge density along the connecting line between two nearest H atoms and along the H–Li line. It confirms that, with

Table 3 Mulliken populations on atoms and shell types for the different types of computation

Basis set	Methods	H				Li			
		Total	s	p	d	Total	s	p	d
A	HF	1.982	1.969	0.013	–	2.018	1.987	0.031	–
	HF+MP2	1.977	1.944	0.033	–	2.023	1.988	0.035	–
B	HF	1.981	1.969	0.012	0.000	2.019	1.987	0.032	–
	HF+MP2	1.978	1.944	0.033	0.001	2.022	1.988	0.034	–
C	HF	1.979	1.966	0.013	0.000	2.021	1.986	0.033	0.002
	HF+MP2	1.975	1.936	0.038	0.001	2.025	1.987	0.035	0.003

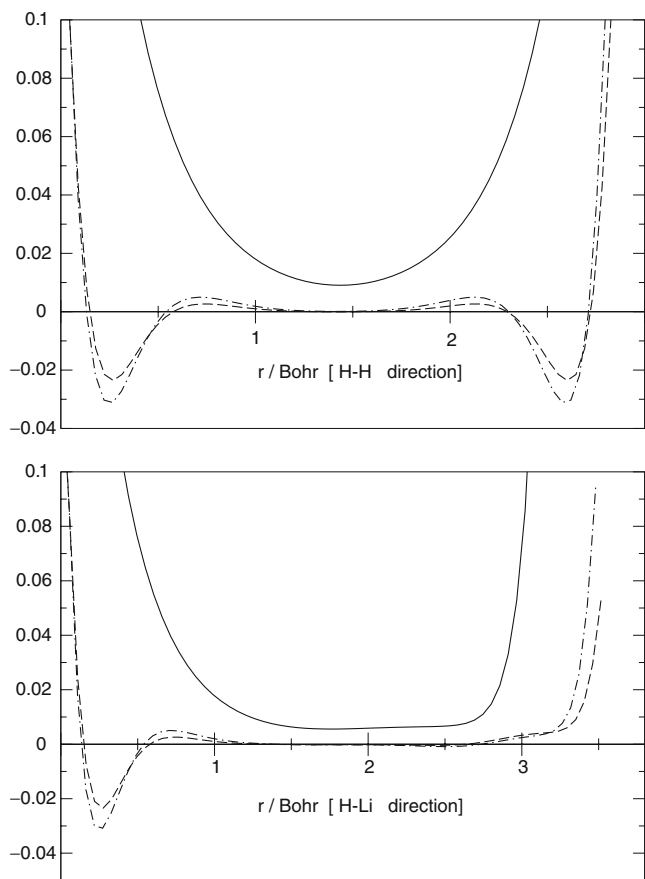


Fig. 4 Profile of the HF density in $|e|/\text{Bohr}^3$ [$\rho^{\text{HF}}(z)$, continuous lines], and of the correcting MP2 density multiplied by a factor 10 [$\rho^{\text{MP2}}(z)$; dashed lines, basis set A; dot-dash lines, basis set C]. The plot above is along a line through the H nuclei in the (110) direction; the plot below is along the line connecting H and Li nuclei in the (100) direction

respect to the HF solution, electrons come slightly closer to the nuclei, as expected, and that there is a small transfer of electrons from H to Li (note the different scales used for the HF density and the MP2 correction). All other effects, including the role of d AOs, are not detectable in these plots.

In order to assess the quality of the calculated charge density, it is convenient to refer to the coefficients of its Fourier transform and compare them with the experimental XSF data. Table 4 reports the results of such an analysis; the calculated data shown there are obtained with basis set C but the following discussion has a general character, because the basis set effects are comparatively negligible. The columns “HF” and “HF + MP2” report the Fourier coefficients F_{hkl}^{calc} of $\rho^{\text{HF}}(\mathbf{r})$ and $\rho^{\text{HF}}(\mathbf{r}) + \rho^{\text{MP2}}(\mathbf{r})$, respectively. It is noted immediately that the (0 0 0) coefficient in the latter case differs from the exact value of four (number of electrons per cell), though by only 0.0025%. This is due to a loss of orthonormality following the periodization of the locally correlated wavefunction (see Ref. [19] for details), but has no important consequence on the other Fourier coefficients. We next observe that the MP2 correction affects only marginally the HF results (the largest contribution is ≈ 0.005 for the (1 1 1) reflexion), and the correction may be either positive or negative. As concerns experimental determinations, we shall refer to the room temperature data by Calder et al. [30] reported in the last column of Table 4: after more than 40 years, this set of 21 XSFs for LiH resulting from very accurate measurements and thoroughly discussed still seems to represent the best available reference. To make comparisons possible, the calculated data must be corrected for thermal motion by applying a Debye–Waller correction separately for electrons associated with the two ionic species. We have simply attributed core band electrons to Li, valence band electrons to the hydride ion. The Debye–Waller factors B_{H} and B_{Li} were optimized in each case so as to minimize the “agreement factor” $R = \sum_{hkl} |f_{hkl}^{\text{obs}} - f_{hkl}^{\text{calc}}| / \sum_{hkl} |f_{hkl}^{\text{obs}}|$. The best fit values resulted $B_{\text{H}} = 1.56 \text{ \AA}^2$, and $B_{\text{Li}} = 0.99$ for both HF and HF+MP2 data, corresponding to R values of 0.01933 and 0.01910, respectively. Using instead the values suggested by Calder et al. [30]: $B_{\text{H}} = 1.80$, $B_{\text{Li}} = 1.01 \text{ \AA}^2$, led to poorer agreement, $R = 0.022$ in the two cases. Much worse results were obtained when

Table 4 Comparison between calculated and observed X-ray structure factors (XSF)

<i>h</i>	<i>k</i>	<i>l</i>	HF	HF + MP2	HF(t)	HF + MP2(t)	Observed
0	0	0	4.00000	3.99902	4.00000	3.99902	4.000
1	1	1	1.05190	1.05631	1.02293	1.02704	1.086 ± 0.002
2	0	0	2.15460	2.15299	2.01674	2.01527	2.032 ± 0.003
2	2	0	1.61270	1.61088	1.42202	1.42050	1.454 ± 0.004
3	1	1	1.08820	1.09206	0.93760	0.94059	0.960 ± 0.004
2	2	2	1.32070	1.31901	1.09773	1.09645	1.096 ± 0.002
4	0	0	1.12220	1.12016	0.87911	0.87769	0.888 ± 0.002
3	3	1	0.86778	0.86893	0.66449	0.66523	0.671 ± 0.005
4	2	0	0.96878	0.96751	0.71560	0.71478	0.738 ± 0.002
4	2	2	0.84846	0.84783	0.59092	0.59056	0.600 ± 0.003
3	3	3	0.69585	0.69568	0.47376	0.47365	0.472 ± 0.006
5	1	1	0.69619	0.69617	0.47393	0.47392	0.474 ± 0.004
4	4	0	0.67117	0.67152	0.41557	0.41572	0.414 ± 0.003
5	3	1	0.56856	0.56796	0.34426	0.34397	0.354 ± 0.001
4	4	2	0.60380	0.60443	0.35252	0.35278	0.349 ± 0.001
6	0	0	0.60388	0.60483	0.35254	0.35295	0.359 ± 0.002
6	2	0	0.54667	0.54771	0.30093	0.30134	0.299 ± 0.001
5	3	3	0.47301	0.47221	0.25475	0.25445	0.248 ± 0.002
6	2	2	0.49761	0.49870	0.25831	0.25869	0.250 ± 0.001
4	4	4	0.45514	0.45615	0.22278	0.22310	0.209 ± 0.002
5	5	1	0.39985	0.39907	0.19158	0.19132	0.182 ± 0.003
7	1	1	0.39985	0.39920	0.19158	0.19136	0.179 ± 0.001

The columns “HF” and “HF+MP2” are referred to the respective calculations with basis set C, and no thermal corrections. The columns “HF(t)” and “HF+MP2(t)” report the same XSFs corrected for thermal motion, using the best-fit Debye–Waller factors $B_{\text{H}} = 1.56 \text{ \AA}^2$, and $B_{\text{Li}} = 0.99 \text{ \AA}^2$. The experimental XSFs by Calder et al. [30] are reported in the last column. See text for discussion

adopting for the Debye–Waller factors the very accurate experimental determinations by Vidal and Vidal-Valat [44] ($B_{\text{H}} = 1.715$, $B_{\text{Li}} = 1.195 \text{ \AA}^2$), giving $R = 0.062$. The value of B_{Li} plays a critical role here by providing too small f values for long reciprocal lattice vectors when it exceeds 1 \AA^2 . Closer inspection reveals that the ineliminable source of the discrepancy lies in the low-index XSFs, where the thermal correction is lowest. In particular the observed value of the (1 1 1) XSF exceeds the calculated one by about 0.06; the MP2 correction apparently accounts for only a tenth of the difference, and it is hard to believe that this is due to inadequate account of correlation effects. It is more likely that the assumption adopted for the thermal correction, implying that the electrons associated to each ion follow rigidly the nuclear motion is hardly applicable in the present case where the motion of ions is relatively large due to their small mass.

Let us finally make some considerations on the effect of correlation corrections on directional CPs and derived quantities. Of particular interest are the auto-correlation functions $B_{[ijk]}(\mathbf{r})$, the Fourier transform of the corresponding directional CPs, since the experimental error has shown to affect them as a damping factor $D(\mathbf{r}) = \exp(-\beta^2 r^2)$, where β is proportional to the resolution in momentum, space. Figure 5 compares the calculated B function along three different directions to

the experimental determination of Ref. [33]. These data confirm first of all the very good agreement between HF and experimental results. It may be questioned whether the residual discrepancies can be attributed to inadequacy of the theoretical (uncorrelated) model or are within experimental errors and numerical accuracies in the computation. This is not clear from the data reported in Fig. 5, which shows that MP2 corrections are of minor importance (note that they are multiplied by a factor ten to make them more visible), exhibit some dependence on basis set, and do not introduce significant improvements in the HF results. This same problem was addressed by Bellaiche and Kunc [45] who performed all-electron calculations for LiH using a plane-wave basis set, and adopting either a local-density Kohn–Sham Hamiltonian or the HF approximation; the calculated CPs were compared with experimental ones from high-resolution X-ray scattering measurements [46]. The agreement was significantly better with HF than with density functional results, which those authors attributed to the fact that HF describes exactly the exchange interaction, while in the other case it is taken into account only approximately. Their general conclusion is that “the effect of the electronic correlation on the CPs in LiH is extremely weak and, for all practical purposes, negligible”. It is probable that also as regards electron distribution in momentum space a

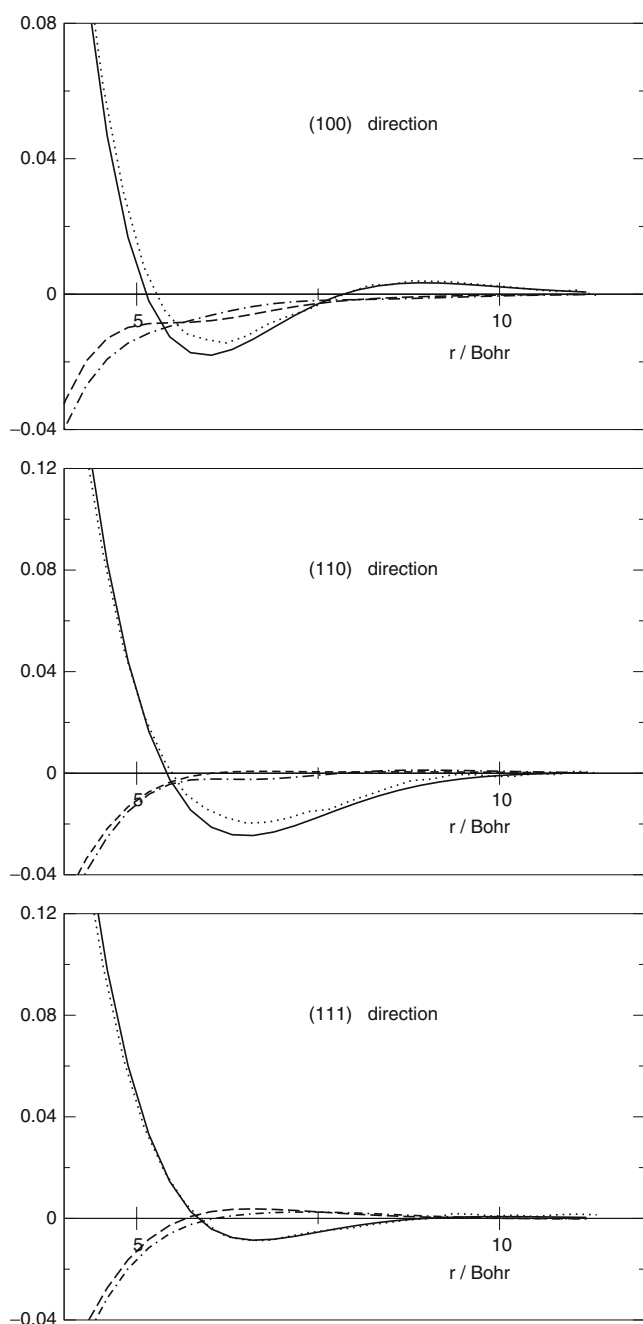


Fig. 5 Calculated autocorrelation function $B_{[ijk]}(\mathbf{r})$ along different directions, as indicated, compared to the experimental determination by Weyrich and Asthalter [33]. All data are corrected with the experimental damping factor $D(\mathbf{r})$. Dotted lines B^{exp} ; continuous lines B^{HF} ; dashed lines B^{MP2} (MP2 correction to the HF data, calculated with the A basis and multiplied by a factor 10); dot-dash lines the same with basis set C

significant role is played by the coupling of nuclear and electronic motions which is totally neglected in the present treatment.

4 Conclusions and prospects

Standard, general-purpose tools for the evaluation of electron correlation effects in crystals using ab initio post-HF methods can represent a useful complement to approaches based on DFT. To implement one such tool is not a trivial task, even if profit can be taken of highly efficient and well tested techniques in current use in molecular quantum chemistry, notably those based on the Locality Ansatz. Crystalline systems present a lot of peculiarities calling for the development of specific algorithms and for the accurate calibration of the computational parameters in order to achieve a satisfactory level of accuracy and efficiency. Among the special requirements we can cite: basis sets adequate to represent the virtual HF manifold while avoiding the risks of quasi-linear dependence; the efficient exploitation of translational and point symmetry; the use of reciprocal space techniques; the correct handling of dispersive interactions up to infinite distance; the size-consistent description of the density matrix.

In the present work we have described a computer code for periodic systems (CRYSCOR) which corrects to second order of perturbation theory the HF solution provided by the CRYSTAL code, using a local correlation method similar to that implemented in the MOLPRO molecular code. The simple case of LiH has been used to document the present capabilities of this approach. It has been shown that good quality computations can be performed at reasonable costs, the main residual problem being that of reaching convergence with respect to basis set size. The correlation correction brings the description of some fundamental quantities such as lattice parameter, cohesive energy, bulk modulus closer to the experiment with respect to HF. The use of the Grimme correction has also been tried, but its usefulness has not yet been proved conclusively. The calculated data concerning the correlated electron distribution (for example, the contraction of the two ions) may also indicate that the MP2 solution is closer to reality than the HF one. However, due to uncertainties affecting the available experimental data (CPs, XSFs) and to the effects of nuclear motion (which is particularly important with the light atoms involved in the present case and is not adequately taken into account) no definite evidence was produced in this respect. New and better experimental data could be very useful; other simple systems with heavier atoms, perhaps MgO or silicon, might be preferable to LiH in order to bring effects of pure electronic correlation to the foreground.

On the theoretical side, the extension to more advanced treatments of the correlation problem in crystals is mandatory; while this task does not present

principal difficulties, it surely requires painstaking and clever work in order to result in an efficient code which can be used to solve problems of real interest. In the meantime, much progress can be achieved and quite a lot of useful experience can be gained even within the MP2 approximation. Work in both directions is being currently carried on.

Acknowledgements We are grateful to Roberto Dovesi for useful discussions and suggestions. Financial support from Italian MURST (Cofin04 Project 25982_002 coordinated by R. Resta) and support from Consorzio INSTM for computer resources at CINECA in the frame of the convention “Super-Progetti di Calcolo” are acknowledged.

References

1. Kristyán S, Pulay P (1994) *Chem Phys Lett* 229:175
2. Pisani C, Busso M, Capocchi G, Casassa S, Dovesi R, Maschio L, Zicovich-Wilson C, Schütz M (2005) *J Chem Phys* 122:094113
3. Pisani C, Dovesi R, Roetti C (1988) Hartree–Fock ab initio treatment of crystalline solids. Lecture notes in chemistry series, vol 48. Springer, Berlin Heidelberg New York
4. Dovesi R, Pisani C, Roetti C, Causà M, Saunders VR (1988) QCPE Program No. 577. Indiana University, Bloomington.
5. Saunders VR, Dovesi R, Roetti C, Orlando R, Zicovich-Wilson CM, Harrison NM, Doll K, Civalleri B, Bush IJ, D’Arco Ph, Llunell M (2003) CRYSTAL03 user’s manual. Università di Torino, Torino
6. Dovesi R, Civalleri B, Orlando R, Roetti C, Saunders VR (2005) *Rev Comp Chem* 21:1
7. Pulay P (1983) *Chem Phys Lett* 100:151
8. Saeb S, Pulay P (1985) *Chem Phys Lett* 113:13
9. Pulay P, Saeb S, Meyer W (1984) *J Chem Phys* 81:1901
10. Werner H-J, Knowles PJ, Schütz M (2002) MOLPRO, version 2002.6. A package of ab initio programs, <http://www.molpro.net>
11. Schütz M, Hetzer G, Werner H-J (1999) *J Chem Phys* 111:5691
12. Schütz M, Lindh R, Werner H-J (1999) *Mol Phys* 96:719
13. Hampel C, Werner H-J (1996) *J Chem Phys* 104:6286
14. Schütz M (2000) *J Chem Phys* 113:9986
15. Johnson ER, DiLabio GA (2006) *Chem Phys Lett* 419:333
16. Grimme S (2003) *J Chem Phys* 118:9095
17. Grimme S (2004) *J Comp Chem* 25:1463
18. Jung Y, Lochan RC, Dutoi AD, Head-Gordon M (2004) *J Chem Phys* 121:9793
19. Pisani C, Casassa S, Maschio L (2006) *Z Phys Chem* 220:913
20. Zicovich-Wilson CM, Dovesi R, Saunders VR (2001) *J Chem Phys* 115:9708
21. Casassa S, Zicovich-Wilson C, Pisani C (2006) *Theor Chem Acc*. DOI 10.1007/s00214-006-0119-z
22. Boughton JW, Pulay P (1993) *J Comput Chem* 14:736
23. Werner H-J, Manby FR, Knowles PJ (2003) *J Chem Phys* 118:8149
24. Schütz M, Manby FR (2003) *Phys Chem Chem Phys* 5:3349
25. Maschio L, Usvjat D, Pisani C, Manby F, Casassa S, Schütz M (2006) *Phys Rev B* (submitted)
26. Usvjat D, Maschio L, Manby F, Schütz M, Casassa S, Pisani C (2006) *Phys Rev B* (submitted)
27. Weyrich W (1998) Quantum-mechanical ab initio calculation of the properties of crystalline materials. In: Pisani C (ed) *Lecture notes in chemistry series, vol 67*. Springer, Berlin Heidelberg New York
28. Islam AKMA (1993) *Phys Status Sol B* 180:9
29. Lebègue S, Alouani M, Arnaud B, Pickett WE (2003) *Eur Lett* 63:562
30. Calder RS, Cochran W, Griffiths D, Lowde DR (1962) *J Phys Chem Sol* 23:621
31. Pattison P, Weyrich W (1979) *J Phys Chem Sol* 40:213
32. Reed WA (1978) *Phys Rev B* 18:1986
33. Weyrich W, Asthalter T (1993) *Z Naturforsch* 48a:303
34. Dovesi R, Ermondi C, Ferrero E, Pisani C, Roetti C (1984) *Phys Rev B* 29:3591
35. Asthalter T, Weyrich W, Harker AH, Kunz AB, Orlando R, Pisani C (1992) *Solid St Comm* 83:725
36. Adams WH (1961) *J Chem Phys* 34:89
37. Gilbert TL (1972) *Phys Rev A* 6:580
38. Kunz AB, Klein DL (1978) *Phys Rev B* 17:4614
39. Boys SF, Bernardi F (1970) *Mol Phys* 19:553
40. Pretzel FE, Gritton GV, Rushing CC, Friauf RJ, Lewis WB, Waldstein P (1962) *J Phys Chem Solids* 23:325
41. Besson JM, Weill G, Hamel G, Nelmes RJ, Loveday JS, Hull S (1992) *Phys Rev B* 45:2613
42. Murnaghan FD (1944) *Proc Acad Sci USA* 30:244
43. Roma G, Bertoni CM, Baroni S (1996) *Sol St Comm* 98:203
44. Vidal JP, Vidal-Valat G (1986) *Acta Cryst B* 42:131
45. Bellaïche L, Kunc K (1997) *Int J Quant Chem* 61:647
46. Gillet JM, Becker PJ, Loupias G (1995) *Acta Cryst A* 51:405